Received: 1 July 2019 | Revised: 11 September 2019 | Accepted: 12 September 2019

DOI: 10.1111/pce.13655

ORIGINAL ARTICLE

WILEY Plant, Cell & Environment

Oryza sativa POSITIVE REGULATOR OF IRON DEFICIENCY RESPONSE 2 (OsPRI2) and OsPRI3 are involved in the maintenance of Fe homeostasis

Huimin Zhang | Yang Li | Mengna Pu | Peng Xu | Gang Liang | Diqiu Yu

CAS Key Laboratory of Tropical Plant Resources and Sustainable Use, Xishuangbanna Tropical Botanical Garden, The Innovative Academy of Seed Design, Chinese Academy of Sciences, Kunming, Yunnan 650223, China

Correspondence
G. Liang, CAS Key Laboratory of Tropical Plant Resources and Sustainable Use, Xishuangbanna Tropical Botanical Garden, The Innovative Academy of Seed Design, Chinese Academy of Sciences, Kunming, Yunnan 650223, China.
Email: lianggang@xtbg.ac.cn

D. Yu, CAS Key Laboratory of Tropical Plant Resources and Sustainable Use, Xishuangbanna Tropical Botanical Garden, The Innovative Academy of Seed Design, Chinese Academy of Sciences, Kunming, Yunnan 650223, China.
Email: ydq@xtbg.ac.cn

Funding information
CAS 135 program, Grant/Award Number: 2017XTBG-T02; Candidates of the Young and Middle Aged Academic Leaders of Yunnan Province, Grant/Award Number: 2015HB095; Applied Basic Research Project of Yunnan Province, Grant/Award Number: 2017FB026

Abstract

Iron (Fe) is an essential micronutrient for plant growth development and plays a key role in regulating numerous cellular processes. In rice, OsHRZ1, an Fe-binding ubiquitin ligase, is a putative sensor of Fe homeostasis that negatively regulates iron acquisition. Despite its apparent importance, only a single basic-Helix–Loop–Helix (bHLH) transcription factor, OsPRI1, has been identified as a direct target of OsHRZ1. In this study, we identified and functionally characterized OsPRI2 and OsPRI3, two paralogs of OsPRI1, observing that they directly interact with OsHRZ1. Additional analyses suggested that OsHRZ1 promotes the degradation of OsPRI2 and OsPRI3. The translocation of Fe from roots to shoots was impaired in plants with loss-of-function mutations in *OsPRI2* or *OsPRI3*, causing the downregulation of Fe-deficiency-responsive genes. In contrast, overexpression of *OsPRI2* and *OsPRI3* promotes Fe accumulation and activates the expression of Fe-deficiency-responsive genes. We also provide evidence that OsPRI2 and OsPRI3 bind to the promoters of *OsIRO2* and *OsIRO3*, two key regulators of Fe homeostasis. Moreover, OsPRI2 and OsPRI3 directly induce expression of the metal-nicotianamine transporter, *OsYSL2*, by associating with the promoter in response to Fe deficiency. Our results provide insights into the complex network regulating Fe homeostasis in rice.

KEYWORDS

iron, OsHRZ1, *OsIRO2*, *OsIRO3*, *OsYSL2*, rice

1 | INTRODUCTION

Because iron (Fe) is involved in many physiological and biochemical processes in plant cells, it is indispensable for growth and development. However, the availability of Fe is very low in alkaline soil. Insufficient Fe restricts chlorophyll biosynthesis, which ultimately leads to chlorotic leaves and decreased crop productivity. Additionally, Fe is highly reactive and potentially toxic because it contributes to the Fenton reaction, which produces hydroxyl radicals that are harmful to cells. Ferrous Fe is abundant in acidic paddy fields under anaerobic conditions, which often results in increased Fe absorption and excessive amounts of Fe in plants (Fageria, Santos, Barbosa, & Guimarães, 2008; Neue, Quijano, Senadhira, & Setter, 1998; Quinet et al., 2012). Thus, Fe toxicity is a severe agricultural problem for crops grown in acidic soil (Quinet et al., 2012). Consequently, Fe homeostasis is tightly controlled in plants.

Higher plants have evolved two major strategies for acquiring Fe (Römheld & Marschner, 1986). Non-graminaceous plants employ a reduction strategy involving the reduction of Fe (III) to Fe (II) and then the transport of Fe (II). In contrast, graminaceous plants use a chelation strategy, which involves the synthesis and secretion of mugineic acid family phytosiderophores, which are Fe (III) chelators (Takagi, 1976). Transcription is a major regulatory step in the maintenance of Fe homeostasis, and Fe deficiency triggers an important transcriptional

reprogramming of cells that switches the basal developmental programs to the necessary Fe-acquisition program (Colangelo & Guerinot, 2004; Li, Zhang, Ai, Liang, & Yu, 2016; Liang, Zhang, Li, Ai, & Yu, 2017; Long et al., 2010; Ogo et al., 2007; Zhang et al., 2015; Zheng et al., 2010). The signaling events that lead to this transcriptional reprogramming are currently being elucidated. In *Arabidopsis thaliana*, FE-DEFICIENCY INDUCED TRANSCRIPTION FACTOR (FIT) is required for the Fe-deficiency response (Colangelo & Guerinot, 2004; Yuan, Zhang, Wang, & Ling, 2005). Specifically, FIT interacts with bHLH38/39/100/101 to activate the expression of the strategy I genes *IRT1* and *FRO2* (Yuan et al., 2008; Wang et al., 2013). Moreover, POPEYE (PYE) maintains Fe homeostasis by negatively regulating the expression of the Fe homeostasis genes *ZIF1*, *FRO3*, and *NAS4* (Long et al., 2010). bHLH105/ILR3 was recently demonstrated to act as a negative regulator of Fe homeostasis by the interaction with PYE (Gao, Robe, Gaymard, Izquierdo, & Dubos, 2019; Tissot et al., 2019) Additionally, *bHLH38/39/100/101* and *PYE* expression levels are upregulated by Fe-deficiency (Long et al., 2010; Wang et al., 2007) in a process that depends on the upstream positive regulators bHLH34/104/105/115 (Li et al., 2016; Liang et al., 2017; Zhang et al., 2015). Fe deficiency responsive signaling is similar across non-graminaceous plants, including soybean, tomato and apple (Li et al., 2018; Ling, Bauer, Bereczky, Keller, & Ganal, 2002; Zhao, Ren, Wang, Wang, et al., 2016; Zhao, Ren, Wang, Yao, et al., 2016).

IRON DEFICIENCY-RESPONSIVE ELEMENT-BINDING FACTOR 1 (IDEF1), which is a central regulator of the rice Fe-deficiency response, can directly bind to Fe, suggesting it is a putative Fe sensor (Kobayashi et al., 2012). It is noteworthy that IDEF1 is essential only for the early response to Fe deficiency, but not for the late response (Kobayashi et al., 2009). The human Fe sensor FBXL5 is degraded when iron sources have been depleted in a process that requires an iron-binding hemerythrin-like domain in its N terminus (Salahudeen et al., 2009; Vashisht et al., 2009). Additionally, FBXL5 is integrated into a complex responsible for the ubiquitination of IRON REGULATORY PROTEIN 2 (IRP2), which is an RNA-binding protein that positively regulates Fe homeostasis in humans (Muckenthaler, Galy, & Hentze, 2008). In *A. thaliana* and rice, BRUTUS (BTS), OsHRZ1, and OsHRZ2 contain the Fe-binding hemerythrin domain and the Really Interesting New Gene (RING) Zn-finger domain, and can bind to iron and exhibit ubiquitination activity (Kobayashi et al., 2013; Long et al., 2010). In addition, two BTS homologs, BTSL1 and BTSL2, also negatively regulate Fe homeostasis in Arabidopsis (Hindt et al., 2017). In *A. thaliana*, the degradation of bHLH105 (also known as ILR3) and bHLH115 is suppressed in the *bts-1* mutant (Selote, Samira, Matthiadis, Gillikin, & Long, 2015). Similarly, OsHRZ1 targets OsPRI1 (a homologue of Arabidopsis bHLH105 and bHLH115) for degradation *via* the 26S proteasome pathway (Zhang, Li, Yao, Liang, & Yu, 2017).

The key signaling events identified so far do not explain how the Fe-deficiency responses are regulated in rice. OsHRZ1 has a close homologue OsHRZ2, and Fe homeostasis regulation is based on a network of transcription factors. OsPRI1 is a key bHLH protein regulating the expression of subsets of Fe-deficiency-responsive genes (Zhang et al., 2017). Because OsPRI1 is the only transcription factor confirmed to be a direct target of OsHRZ1, additional transcription factors targeted by OsHRZ1 will need to be identified.

In the present study, we identified OsPRI2 and OsPRI3 as two paralogs of OsPRI1, both of which interact with OsHRZ1. Loss-of-function mutations to each of these two transcription factors resulted in severe Fe-deficiency symptoms, inhibited Fe translocation from the roots to the shoots, and downregulated expression of Fe-deficiency-responsive genes. In contrast, the overexpression of these genes promoted Fe accumulation in the roots and shoots and enhanced the expression of Fe-deficiency-responsive genes. Furthermore, the downstream genes *OsIRO2/3* and *OsYSL2* were directly regulated by OsPRI2 and OsPRI3.

2 | MATERIALS AND METHODS

2.1 | Plant materials and growth conditions

Cultivar 'Nipponbare' was used in the study. *hrz1–2* mutant was described previously (Zhang et al., 2017). For hydroponic culture assays, plants were grown in a greenhouse with a photoperiod of 14 h light and 10 h dark at 28°C. Fe-sufficient liquid media was prepared in 1/2 MS with 0.1 mM Fe (III)-EDTA and Fe-deficient liquid media in 1/2 MS without Fe.

2.2 | Yeast-two-hybrid assay

For the yeast-two-hybrid assay, GBK-OsHRZ1-C and GAD-OsPRI1 were reported previously (Zhang et al., 2017), and the full-length CDS of OsPRI2/3 was cloned into pGADT7. Primers used for plasmid construction were listed in Supplemental Table S1. Yeast growth was determined as described in the Yeast Two-Hybrid System User Manual (Clontech).

2.3 | Pull-down assay

Full-length OsHRZ1 and OsPRI2/3 were cloned into pGEX-4 T-1 and pET-28a (+), respectively. All plasmids were introduced into *Escherichia coli* BL21 cells (TransGen Biotech). GST, GST-OsHRZ1, and His-OsPRI2/3 proteins were induced by 0.1 mM isopropyl-b-thiogalactopyranoside (IPTG) at 16°C for 24 h. Soluble GST and GST-OsHRZ1 were extracted and immobilized to glutathione affinity resin (Thermo Fisher Scientific). For pull-down assays, His-OsPRI2/3 fusion proteins from *E. coli* cell lysate were incubated with the immobilized GST and GST-OsHRZ1 proteins in PBS buffer (50 mM Tris–HCl, pH 7.2, 150 mM NaCl, 10% glycerol, 0.1% Triton X-100, 1 × protease inhibitor cocktail from Roche) for 2 h at 4°C. Proteins were eluted in the elution buffer, and the interaction was determined by western blot using anti-His antibody (TransGen Biotech).

2.4 | Construction of plasmids

To ensure the gene targeting efficiency and avoid off-targets, target sites were designed by the use of CRISPR-GE (http://skl.scau.edu.cn/; Xie et al., 2017). The editing vectors were constructed as described previously (Liang, Zhang, Lou, & Yu, 2016). Briefly, for the editing of *OsPRI2* and *OsPRI3*, the OsU6a promoter driving the sgRNA containing a single target site was cloned into the pMH-SA vector by the restriction enzyme sites *Spe*I and *Asc*I (Liang et al., 2016). For the double editing of *OsIRO2*, two target sites driven by *OsU6a* and *OsU6b* promoters respectively were subcloned into pSAK2 and further transferred to pMH-SA by the restriction enzyme sites *Spe*I and *Asc*I. Homozygous mutant lines were identified by sequencing.

For the construction of overexpression vectors, the HA-OsPRI2/3 fusion sequences were obtained from the GAD-OsPRI2/3 vectors and cloned between the maize ubiquitin promoter and the NOS terminator in the pUN1301 binary vector.

2.5 | Transient expression assays in tobacco

Agrobacterium tumefaciens strain EHA105 was used in the transient expression experiments. Infiltration assays were performed as described previously (Liu et al., 2010). The binary vector pOCA30 containing a *35S* promoter and a polyA termination was used for construction of *35S:GFP*, *35S:OsHRZ1-GFP* and *35S:OsPRI2/3-GFP*. Briefly, the strains were first plated on LB medium containing the appropriate selection antibiotics. After 2–3 d, a single colony was inoculated into 5 mL LB medium supplemented with the appropriate antibiotics and grown at 28°C in a shaker for 48 h. The culture was transferred to new 50 mL LB medium with the appropriate antibiotics. When growth reached an OD600 of approximate 3.0, the bacteria were spun down gently (3200 *g*, 5 min), and the pellets were resuspended in infiltration buffer (10 mM $MgCl_2$, 10 mM MES, pH 5.6) at a final OD600 of 1.5. A final concentration of 0.2 mM acetosyringone was added and the bacteria were kept at room temperature for at least 2 h without shaking. For co-infiltration of the 3 different combinations (a, *OsHRZ1-GFP*: *OsPRI2/3-GFP*: *GFP*: empty vector = 0: 10: 5: 20; b, *OsHRZ1-GFP*: *OsPRI2/3-GFP*: *GFP*: empty vector = 10: 10: 5: 10; c, *OsHRZ1-GFP*: *OsPRI2/3-GFP*: *GFP*:empty vector = 20: 10: 5: 0), the agrobacterium strains carrying different constructs were mixed prior to infiltration. Leaf infiltration was conducted in 3-week-old *N. benthamiana* by pressing a 1 mL disposable syringe to the surface of fully expanded leaves. Protein extraction and immunoblot were conducted as described previously (Liu et al., 2010). Anti-GFP antibody (Affinity Biosciences) was used.

2.6 | CoIP assay

The indicated proteins were transiently expressed in the *N. benthamiana* leaves. The leaves were infiltrated with MG132 12 hours before harvesting. The samples of 1 g leaves were freeze ground to powder and homogenized.

in 2 mL IP buffer (50 mM Tris–HCl, pH 7.4, 150 mM NaCl, 1 mM MgCl2, 20% glycerol, 0.2% NP-40, 1 X protease inhibitor cocktail and 1 X phosphatase inhibitor cocktail from Roche). Lysates were clarified by centrifugation at 20 000 *g* for 15 min at 4°C and were incubated with GFP-Trap agarose beads (ChromoTek) for 4 h at 4°C in a top to end rotator. After incubation, the beads were washed five times with ice-cold washing buffer (50 mM Tris–HCl, pH 7.4, 150 mM NaCl, 1 mM $MgCl_2$, 20% glycerol and 0.02% NP-40) and then eluted by boiling in reducing SDS sample buffer. Samples were separated by SDS–PAGE and analysed by immunoblot using anti-GFP and anti-HA antibody (Affinity Biosciences).

2.7 | Immunoblotting

For total protein extraction, roots were ground to a fine powder in liquid nitrogen and then resuspended and extracted in RIPA buffer (50 mM Tris, 150 mM NaCl, 1% NP-40, 0.5% sodium deoxycholate, 0.1% SDS, 1 mM PMSF, 1 X protease inhibitor cocktail [pH 8.0]). Isolation of cytoplasmic and nuclear proteins was performed as described previously (Li et al., 2018). Sample was loaded onto 12% SDS-PAGE gels and transferred to nitrocellulose membranes. The membrane was blocked with TBST (10 mM Tris-Cl, 150 mM NaCl, and 0.05% Tween 20, pH 8.0) containing 5% nonfat milk (TBSTM) at room temperature for 60 min and incubated with primary antibody in TBSTM (overnight at 4°C). Membranes were washed with TBST (three times for 5 min each) and then incubated with the appropriate horseradish peroxidase-conjugated secondary antibodies in TBSTM at room temperature for 1.5 h. After washing three times, bound antibodies were reacted with ECL substrate and visualized by a chemiluminescence reader (Tanon-5200).

2.8 | Gene expression analysis

Total RNA was extracted using the Trizol reagent (Invitrogen). For the reverse transcription reaction, 1 μg total RNA was used for cDNA synthesis by oligo (dT)18 primer according to the manufacturer's protocol (Takara). The resulting cDNA was subjected to relative quantitative PCR using the SYBR Premix Ex Taq kit (TaKaRa) on a Roche LightCycler 480 real-time PCR machine, according to the manufacturer's instructions. *OsACTIN1* was amplified as an internal control, and gene copy number was normalized to that of *OsACTIN1*. For the quantification of each gene, at least three biological replicates were used. Each biological replicate contained three technical replicates. The quantitative reverse transcription-PCR primers are listed in Supplemental Table S1.

2.9 | Fe concentration measurement

To determine Fe concentration, 7-day-old seedlings grown in 1/2 MS liquid with 0.1 mM Fe (III)-EDTA were transferred to Fe-sufficient (0.1 mM Fe (III)-EDTA) or Fe-deficient (Fe free) liquid media for 7 d. The shoots (the whole overground part) and roots were harvested

separately and dried at 65°C for 3 d. For each sample, about 100 mg dry weight of roots or shoots was wet-ashed with 1.5 mL of 11 M HNO_3 and 1.5 mL of 8.8 M H_2O_2 for 20 min at 220°C. Metal concentrations were measured using Inductively Coupled Plasma Mass Spectrometry (ICP-MS). Three biological replicates were used for Fe concentration analysis.

2.10 | ChIP-qPCR assay

ChIP assays were performed essentially according to previously described protocols (Saleh, Alvarez-Venegas, & Avramova, 2008). Seven-day-old plants (wild-type, *OsPRI2-OX-5*, *OsPRI3-OX-7*) grown on +Fe media were shifted to –Fe media for 1 week and roots were harvested for ChIP assays. To quantify OsPRI2/3-DNA binding, qPCR was performed according to the procedure described previously with the *pOsACTIN1* as the endogenous control. All primers are listed in Supplementary Table S1. For the quantification of each DNA fragment, three biological replicates were used.

2.11 | EMSA

A Chemiluminescent EMSA Kit (Beyotime) was used to conduct EMSA following the manufacturer's protocol. The recombinant GST-OsPRI2/3 protein and GST protein were purified from *E. coli*. The DNA fragments of the promoters were obtained by annealing two complementary oligonucleotides which were synthesized and labeled with/without biotin at the 5′ terminal. Biotin-unlabeled fragments of the same sequences or mutated sequences were used as competitors, and the GST protein alone was used as the negative control.

2.12 | Cell-free degradation assays

Fresh rice roots were ground into fine powder in liquid nitrogen and then used for total proteins extraction in a degradation buffer (25 mM Tris–HCl, pH 7.5, 10 mM NaCl, 10 mM $MgCl_2$, 4 mM PMSF, 5 mM DTT, and 10 mM ATP) as previously described (Wang et al., 2009). After two 10 min centrifugations at 17 000 *g* in 4°C, cell debris was removed. The supernatant was collected and protein concentration was examined by the Bio-Rad protein assay. To inhibit the 26S proteasome pathway, 40 μM MG132 was added to the degradation buffer as indicated. GST-OsPRI2/3 proteins were expressed and purified from *E. coli* 100 ng of recombinant protein was incubated in 0.1 mL extracts (containing 500 μg total proteins) for the individual assays. All the mock controls used an equal amount of solvents for each drug. The extracts were incubated at 28°C, and samples were taken at indicated intervals for determination of recombinant protein abundance by immunoblots.

3 | RESULTS

3.1 | OsHRZ1 promotes the degradation of OsPRI2 and OsPRI3

We previously revealed that OsPRI1 controls the Fe-deficiency response and is directly targeted by OsHRZ1. A comparison of sequences indicated that OsPRI2 (Os05g0455400, OsbHLH58) and OsPRI3 (Os02g0116600, OsbHLH59) are paralogs of OsPRI1 (Figure S1). A yeast two-hybrid assay was used to test the putative interactions of OsPRI2 and OsPRI3 with OsHRZ1. Specifically, *OsPRI2* and *OsPRI3* were fused in frame with the GAL4 activation domain in the pT7GAD vector. Meanwhile, the sequence encoding the C-terminus of OsHRZ1 was fused to the sequence encoding the GAL4 DNA-binding domain in the pT7GBK vector. The interaction between OsPRI1 and OsHRZ1 was used as a positive control. As expected, OsPRI2 and OsPRI3 interacted with OsHRZ1 in yeast cells (Figure 1a).

To verify that OsPRI2 and OsPRI3 are directly targeted by OsHRZ1, we performed pull-down experiments involving the following purified recombinant fusion proteins: GST-HRZ1 (glutathione S-transferase-OsHRZ1), His-OsPRI2 (6× histidine-OsPRI2), and His-OsPRI3. The interactions based on the results of the pull-down experiments were consistent with those observed in yeast cells (Figure 1b). The OsPRI2 and OsPRI3 proteins could be pulled down by GST-HRZ1. A co-immunoprecipitation (CoIP) assay further confirmed that OsHRZ1 interacted with OsPRI2 and OsPRI3 in plant cells (Figure 1c).

We previously confirmed that OsHRZ1 mediates the degradation of OsPRI1 *via* the 26S proteasome. In this study, we analysed whether the stability of the OsPRI2 and OsPRI3 proteins is also controlled by OsHRZ1. Thus, vectors carrying the OsHRZ1-GFP and OsPRI2/3-GFP constructs were infiltrated into the same *Nicotiana benthamiana* leaf area according to an *Agrobacterium tumefaciens*-mediated transformation method. Samples were then analysed in a western blot experiment (Figures 1d & S2). As the amount of OsHRZ1-GFP increased, the abundance of the OsPRI2-GFP and OsPRI3-GFP proteins decreased. Regarding the control, the GFP protein level was similar in all samples.

We applied cell-free degradation assays to monitor the degradation of OsPRI2 and OsPRI3 (Figure 1e). When incubated with total protein extracts from wild-type roots, both proteins were obviously degraded. In contrast, when incubated with the total protein extracts from *hrz1–2* mutant roots, both proteins were only slightly degraded. Their degradation was inhibited by carbobenzoxyl-leucinyl-leucinyl-leucinal (MG132), which is a 26S proteasome inhibitor. These data suggest that OsPRI2 and OsPRI3 are degraded in an OsHRZ1-dependent manner *via* the 26S proteasome pathway.

3.2 | Loss-of-function mutations to *OsPRI2* and *OsPRI3* impair Fe translocation from the roots to the shoots

Considering that OsPRI2 and OsPRI3 may help regulate Fe homeostasis, we determined whether the expression of the corresponding

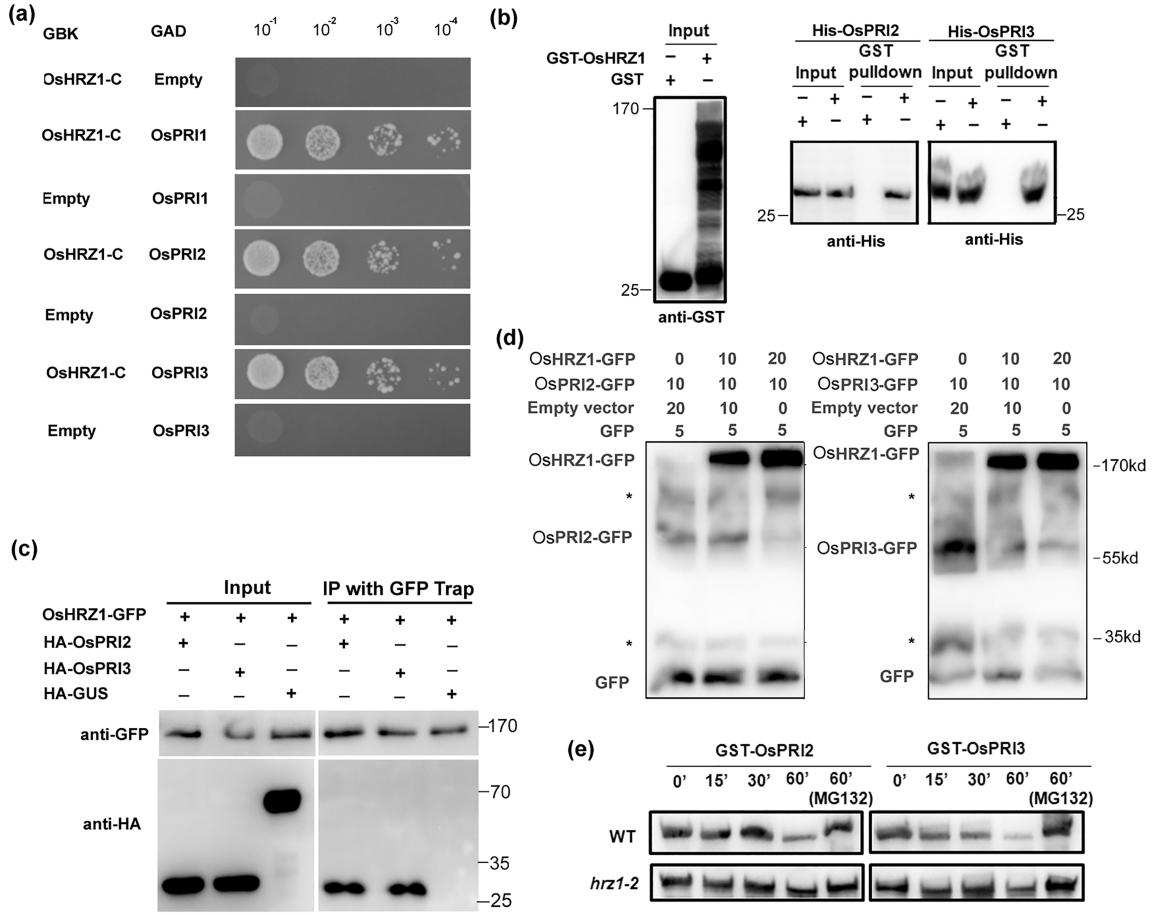

FIGURE 1 Interaction of OsHRZ1 with OsPRI2 and OsPRI3. (a) Yeast two-hybrid assays. Yeast co-transformed with different BD and AD plasmid combinations were spotted in parallel in 10-fold dilution series on synthetic dropout medium lacking Leu/Trp/His/Ade. The C-terminal truncated OsHRZ1 and full-length OsPRI2/3 were cloned into pGBKT7 and pGADT7, respectively. OsHRZ1-C/OsPRI1, positive control. OsHRZ1-C/Empty, negative control. (b) Pull-down assay. OsHRZ1 was fused with the GST tag and OsPRI2/3 were fused with the His tag. Recombinant proteins were expressed in *E. coli*. Proteins were pulled down by glutathione Sepharose 4B and detected using the anti-His antibody. Protein molecular weight (in kDa) is indicated. (c) CoIP assay. Total proteins from different combinations with OsHRZ1-GFP and HA-OsPRI2/HA-OsPRI3/HA-GUS were immunoprecipitated with GFP-Trap followed by immunoblotting with the indicated antibodies. HRZ1-GFP/HA-GUS, negative control. Protein molecular weight (in kDa) is indicated. (d) Degradation of OsPRI2 or OsPRI3 was carried out by detecting the OsPRI2/3-GFP protein level in co-infiltration experiments with increasing amounts of OsHRZ1-GFP. GFP proteins were used as an internal control. Anti-GFP antibody was used in western blot. Protein molecular weight (in kDa) is indicated. Stars indicate the non-specific bands. Numbers indicate the ratio of the concentrations of agrobacteria used in co-infiltration. Empty vector, a binary vector pOCA30 with a 35S promoter; GFP, 35S:GFP in pOCA30; OsPRI2-GFP, 35S:OsPRI2-GFP in pOCA30; OsPRI3-GFP, 35S:OsPRI3-GFP in pOCA30; OsHRZ1-GFP, 35S:OsHRZ1-GFP in pOCA30. (e) Cell-free degradation. Ten-day-old roots grown in Fe-sufficient solution were harvested and used for protein extraction. Incubation with or without MG132 was performed over the indicated time course

genes is responsive to Fe deficiency. We observed that the root and shoot *OsPRI2* and *OsPRI3* expression levels were similar under Fe-deficient or -sufficient conditions (Figure S3). We then examined their expression patterns among the different parts of plants, finding that *OsPRI2* was preferentially expressed in the overground part and *OsPRI3* had the highest expression in the roots (Figure S4). To functionally characterize *OsPRI2* and *OsPRI3*, a CRISPR/Cas9 system was employed to edit both genes. To produce loss-of-function mutants, we targeted sites within DNA regions corresponding to the bHLH domain for an insertion or deletion mutation. The homozygous *pri2–1* and *pri2–2* mutants contained 4 BP and 49 BP deletions, respectively, while the homozygous *pri3–1* and *pri3–2* mutants had a 4 bp deletion and a 1 BP insertion, respectively (Figure 2a). These changes were predicted to cause frame-shift mutations in the bHLH domain. We then phenotypically analysed the mutants grown in Fe-sufficient and Fe-deficient conditions (Figure 2b). Regardless of Fe status, both the *pri2* and *pri3* mutants developed shorter shoots than wild-type control (Figures 2b & S5a). Under Fe-deficient conditions, the *pri2* and *pri3* mutants produced significantly shorter roots and shoots compared with the wild-type control (Figures 2b & S5a). We then measured the Fe concentrations of the roots and shoots (Figure 2c). The root Fe concentration was consistently higher in the mutants than in the wild-type control, whereas the opposite pattern was observed for the shoot Fe concentration, regardless of the external Fe status. Moreover, seed Fe concentration was also lower in the mutants than in the wild type (Figure S5b).

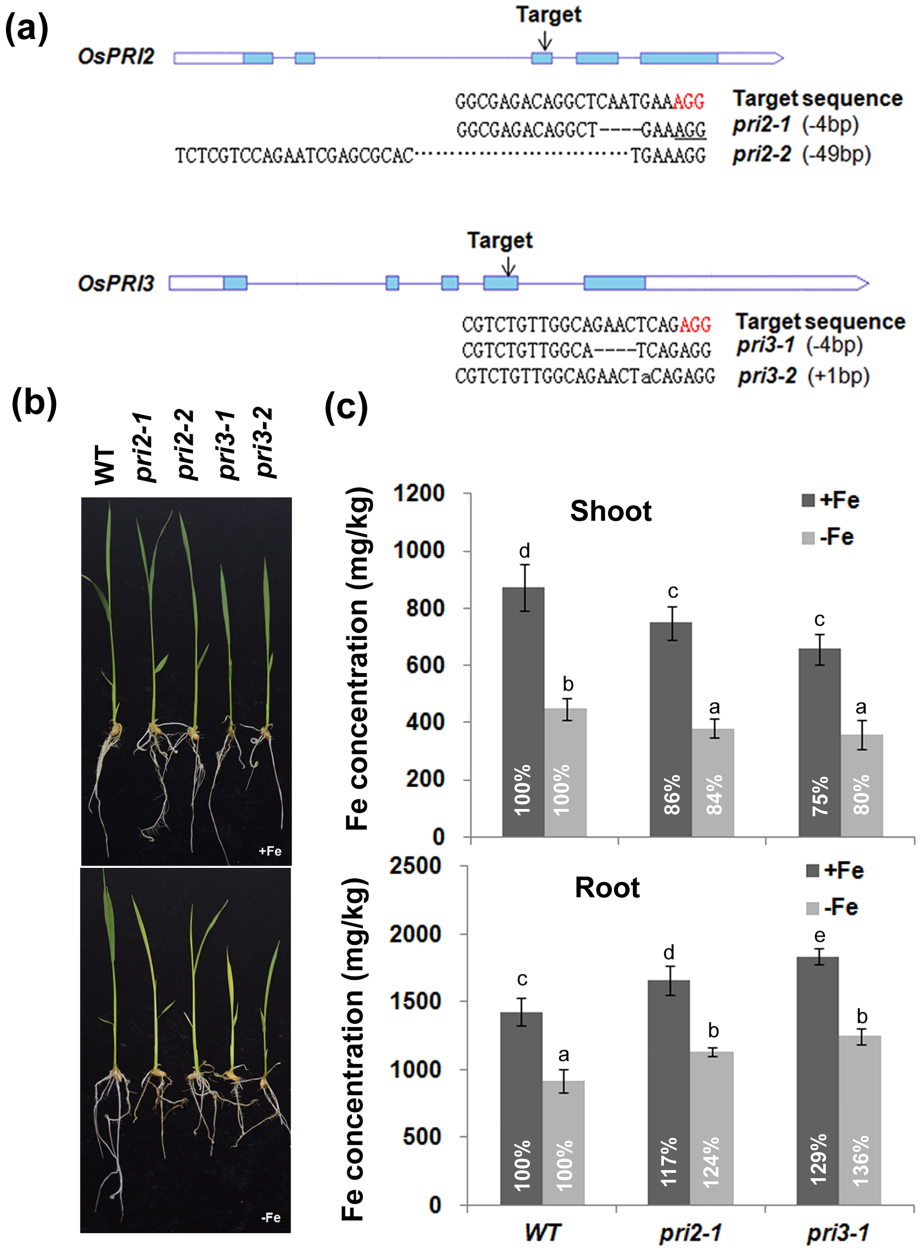

FIGURE 2 Phenotypes of *pri2* and *pri3* mutants. (a) Mutations in the *pri2* and *pri3* mutants. The arrows indicate the positions of target sites. The red nucleotides indicate the PAM region recognized by CRISPR/Cas9 system. (b) Phenotypes of 10-day-old seedlings. Three-day-old seedlings germinated in wet paper were shifted to Fe-sufficient or Fe-deficient hydroponic media for 7 d. (c) Fe concentration. Two-week-old seedlings grown in Fe-sufficient media were transferred to Fe-sufficient or Fe-deficient media for 1 week. Shoots and roots were separately sampled and used for metal measurement. Three biological replicates were performed. The percentage of each value relative to the value in wild type is shown. The different letters above each bar indicate statistically significant differences as determined by one-way ANOVA analysis followed by Tukey's multiple test ($P < 0.05$) [Colour figure can be viewed at wileyonlinelibrary.com]

3.3 | Loss-of-function mutations to *OsPRI2* and *OsPRI3* downregulate expression of Fe-deficiency-responsive genes

Both OsPRI2 and OsPRI3 are transcription factors. On the basis of the observed disrupted Fe homeostasis due to loss-of-function mutations to *OsPRI2* and *OsPRI3*, we speculated these two transcription factors may regulate the expression of Fe-deficiency-responsive genes. In rice, *OsNAS1* and *OsNAS2* which are responsible for the synthesis of nicotianamine (NA), are sensitive to Fe availability, with low Fe levels considerably upregulating their expression (Inoue et al., 2003). However, their expression decreased significantly in the *pri2* and *pri3* mutants (Figure 3). Additionally, OsYSL2 and OsYSL15 are responsible for the transport of Fe, and the expression levels of the corresponding genes are upregulated under Fe-deficient conditions (Inoue et al., 2009; Ishimaru et al., 2010; Koike et al., 2004; Lee et al., 2009). As expected, *OsYSL2* and *OsYSL15* expression levels were lower in the *pri2* and *pri3* mutants than in the wild-type control (Figure 3). *OsIRO2*

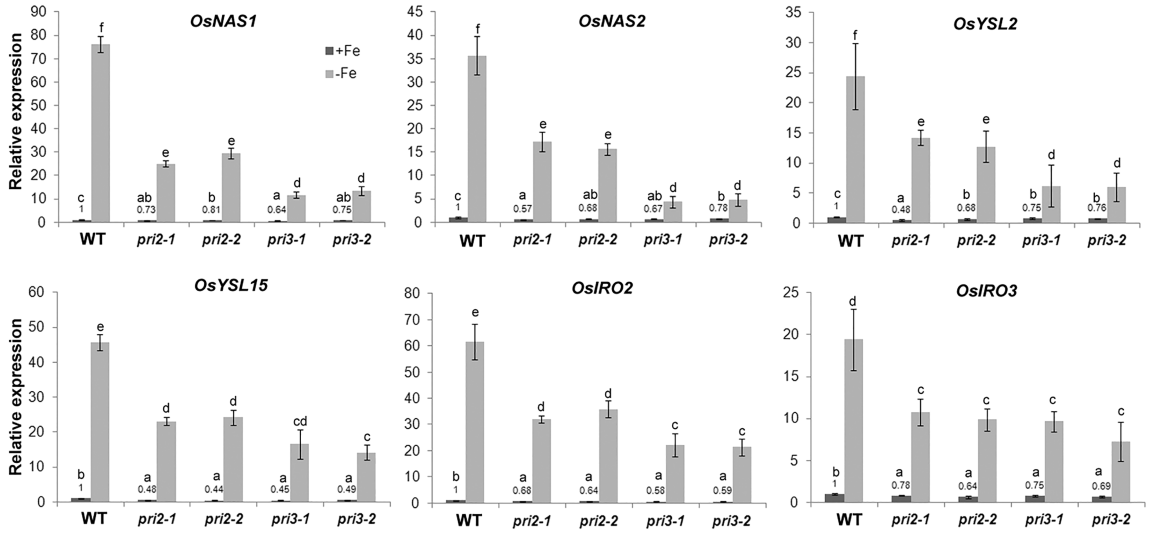

FIGURE 3 Expression of Fe-deficiency responsive genes in the *pri2* and *pri3* mutants. Seven-day-old seedlings grown in Fe-sufficient media were transferred to Fe-sufficient or Fe-deficient media for 7 d. Roots were sampled and used for RNA extraction. The numbers above the bars indicate the corresponding mean values. Three biological replicates were performed. The different letters above each bar indicate statistically significant differences as determined by one-way ANOVA analysis followed by Tukey's multiple test ($P < 0.05$)

encodes a positive regulator, while *OsIRO3* encodes a negative regulator, of Fe homeostasis (Ogo et al., 2007; Zheng et al., 2010). We observed that the *OsIRO2* and *OsIRO3* expression levels were significantly lower in the *pri2* and *pri3* mutants than in the wild-type control (Figure 3). These results suggested that the expression of Fe-deficiency-responsive genes is positively regulated by OsPRI2 and OsPRI3.

3.4 | Overexpression of *OsPRI2* and *OsPRI3* results in increased Fe accumulation

To further clarify OsPRI2 and OsPRI3 functions, we generated transgenic plants in which HA-tagged *OsPRI2* and *OsPRI3* open reading frames were overexpressed under the control of the maize ubiquitin promoter. A quantitative real-time polymerase chain reaction (qRT-PCR) analysis indicated that *OsPRI2* and *OsPRI3* mRNA levels were significantly higher in transgenic plants than in the wild-type control (Figure S6). We then examined how the transgenic plants were affected by the Fe status (Figure 4a). When grown under Fe-sufficient conditions, the shoots of the *OsPRI2*-overexpressing (*OX*) and *OsPRI3-OX* plants were similar to the wild-type, while the *OsPRI2-OX* root lengths were shorter than the wild-type (Figures 4a & S7a). When grown under Fe-deficient conditions, the roots of the *OsPRI2-OX* plants were shorter than the wild-type, but the roots and shoots of the *OsPRI3-OX* plants were longer than the wild-type roots (Figures 4a & S7a). Moreover, we examined the Fe concentrations of the transgenic plants. The Fe concentrations of the roots, shoots and seeds were consistently higher in the transgenic plants than in the wild-type control (Figures 4b & S7b). These data suggested that the overexpression of *OsPRI2* and *OsPRI3* leads to the increased Fe uptake.

3.5 | Overexpression of *OsPRI2* or *OsPRI3* upregulates expression of Fe-deficiency-responsive genes

The observed increased Fe accumulation in the transgenic plants may have been due to the upregulated expression of genes associated with Fe uptake. Therefore, we examined the expression of Fe-deficiency-responsive genes in the transgenic plants. One-week-old seedlings grown in hydroponic medium with sufficient Fe were transferred to the same medium with or without sufficient Fe and incubated for another week. The roots were harvested for a subsequent RNA extraction. The expression levels of six Fe-deficiency-responsive genes (*OsNAS1*, *OsNAS2*, *OsYSL2*, *OsYSL15*, *OsIRO2*, and *OsIRO3*) were significantly upregulated in the transgenic plants regardless of Fe availability (Figure 5). These data implied that OsPRI2 and OsPRI3 positively regulate the expression of Fe-deficiency-responsive genes.

3.6 | OsPRI2 and OsPRI3 bind to the *OsIRO2* and *OsIRO3* promoters

The Fe-deficiency-responsive genes include *OsIRO2* and *OsIRO3*, which encode two key transcription factors that mediate Fe homeostasis. The former positively regulates (Ogo et al., 2007), while the latter negatively regulates (Zheng et al., 2010), the expression of the downstream Fe-deficiency-responsive genes. Because the expression of *OsIRO2* and *OsIRO3* was positively correlated with OsPRI2 and OsPRI3, we examined whether these transcription factors directly regulate the expression of *OsIRO2* and *OsIRO3*. The putative *OsIRO2* and *OsIRO3* promoter regions comprise several E-box motifs (CANNTG) (Figure 6a), which are usually recognized by

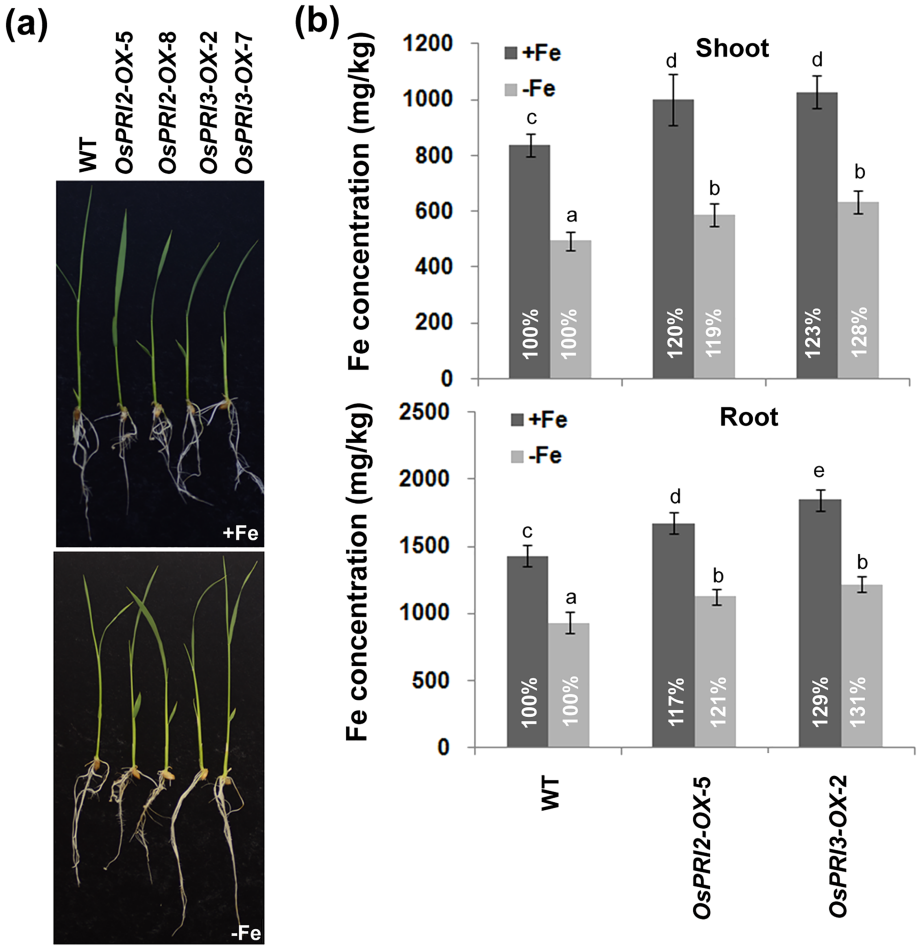

FIGURE 4 Phenotypes of overexpression plants. (a) Phenotypes of 10-day-old seedlings. Three-day-old seedlings germinated in wet paper were shifted to Fe-sufficient or Fe-deficient hydroponic media for 7 d. (b) Two-week-old seedlings grown in Fe-sufficient media were transferred to Fe-sufficient or Fe-deficient media for 1 week. Shoots and roots were separately sampled and used for metal measurement. Three biological replicates were performed. The percentage of each value relative to the value in wild type is shown. The different letters above each bar indicate statistically significant differences as determined by one-way ANOVA analysis followed by Tukey's multiple test ($P < 0.05$) [Colour figure can be viewed at wileyonlinelibrary.com]

bHLH transcription factors (Fisher & Goding, 1992). To investigate the potential association of OsPRI2/3 with the promoters of *OsIRO2/3*, ChIP-qPCR experiments were performed (Figure 6 b). These assays revealed that the promoter sequences of *OsIRO2/3* spanning E-box motifs were highly enriched in anti-HA-immunoprecipitated chromatin in the *OsPRI2-OX* and *OsPRI3-OX* plants compared with wild type. To further explore the possible DNA-binding activity of OsPRI2 and OsPRI3, we conducted an electrophoresis mobility shift assay (EMSA) (Figure 6c). Specifically, GST-OsPRI2 and GST-OsPRI3 fusion proteins produced in *Escherichia coli* cells were purified, and DNA probes (Cold-Probe, Cold-Probe-m, and Biotin-Probe) were synthesized. Both GST-OsPRI2 and GST-OsPRI3 could bind to the Biotin-Probe. In contrast, GST alone was unable to bind to the Biotin-Probe. Meanwhile, the binding between the fusion proteins and the Biotin-Probe was inhibited by the addition of increasing amounts of the unlabeled wild-type probes (Cold-Probe), but not the mutated probes (Cold-Probe-m). These data suggested that OsPRI2 and OsPRI3 can bind to the *OsIRO2* and *OsIRO3* promoters.

3.7 | *OsYSL2* is targeted by OsPRI2 and OsPRI3

Among the Fe-deficiency-responsive genes, *OsYSL2*, which encodes a metal-nicotianamine transporter, is responsible for the long-distance transport of Fe. A previous study concluded that in *OsYSL2* RNAi transgenic plants, the Fe concentration increases in the roots, but decreases in the shoots (Ishimaru et al., 2010), suggesting the Fe translocation from the roots to the shoots is disrupted. The observed downregulated expression of *OsYSL2* in the *pri2* and *pri3* mutants might account for the impaired Fe distribution between the roots and shoots.

Another earlier study confirmed that the *OsNAS1*, *OsNAS2*, and *OsYSL15* expression levels are positively regulated by OsIRO2 (Ogo et al., 2007). In contrast, the expression of *OsYSL2* is not controlled by OsIRO2 (Ogo et al., 2011). We used a CRISPR/Cas9 system to generate two independent *iro2* mutants, both of which contained the same 119 BP deletion in the predicted bHLH domain (Figure S8). Under Fe-sufficient conditions, no visible phenotypic difference was observed between the wild-type control and the *iro2* mutants.

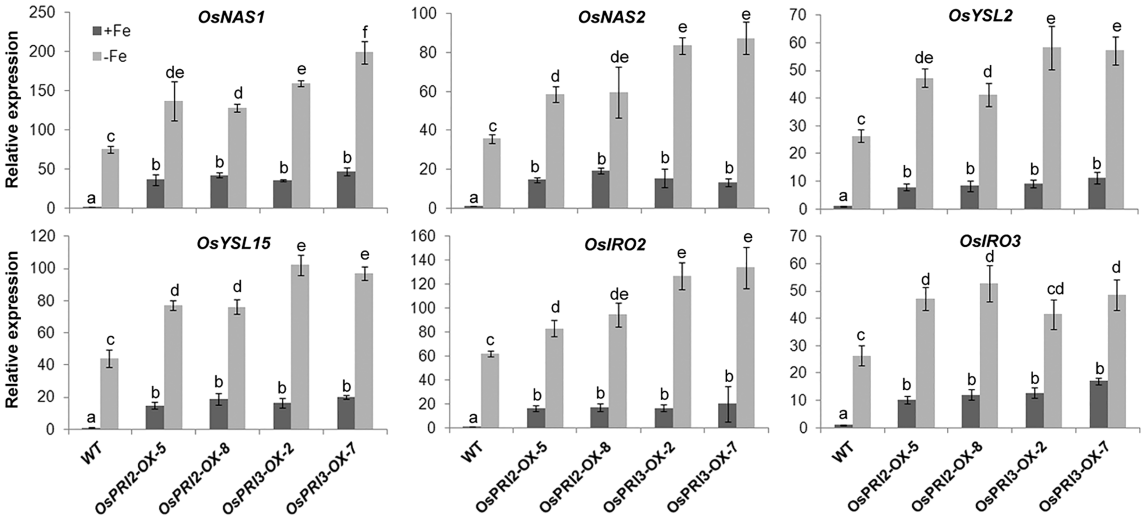

FIGURE 5 Expression of Fe-deficiency responsive genes in the overexpression plants. Seven-day-old seedlings grown in Fe-sufficient media were transferred to Fe-sufficient or Fe-deficient media for 7 d. Roots were sampled and used for RNA extraction. The numbers above the bars indicate the corresponding mean values. Three biological replicates were performed. The different letters above each bar indicate statistically significant differences as determined by one-way ANOVA analysis followed by Tukey's multiple test ($P < 0.05$)

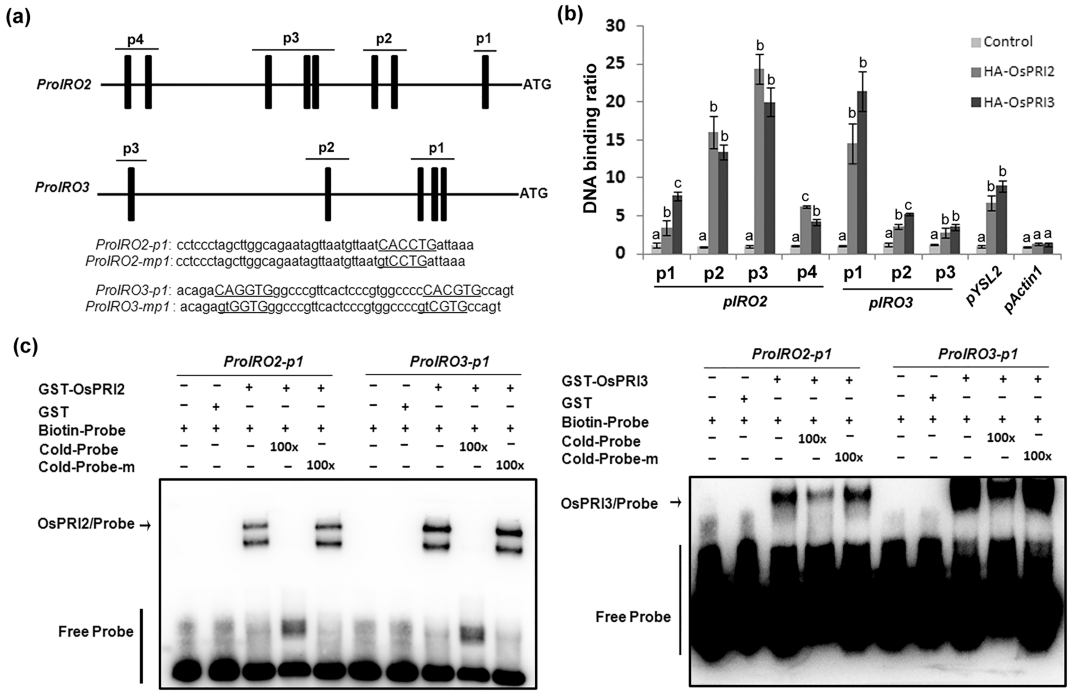

FIGURE 6 OsPRI2 and OsPRI3 bind to the promoters of *OsIRO2* and *OsIRO3*. (a) Position of E-boxes. The bar indicates the position of E-box in the 1.5 kbp sequence from the translation start site of *OsIRO2* and *OsIRO3*. The oligonucleotides (*OsIRO2/3-p1* and *OsIRO2/3-mp1*) were used as the probes in (c). The underlined lower-case base indicates the mutated base. (b) ChIP-qPCR analyses of the DNA binding ratio of OsPRI2/3 to the promoters of *OsIRO2/3* and *OsYSL2* genes. qPCR was used to quantify enrichment of the indicated promoters and a fragment of the *OsACTIN1* promoter containing an E-box motif was used as a negative control. The DNA binding ratio indicates the targeted DNA fragment levels relative to the *OsACTIN1* promoter fragment in the control (wild-type plants). The different letters above each bar indicate statistically significant differences as determined by one-way ANOVA analysis followed by Tukey's multiple test ($P < 0.05$). (c) EMSA assays. Each biotin-labeled DNA probe was incubated with the recombinant GST-OsPRI2/3 protein. An excess of unlabeled probe (Cold-Probe) or labeled mutated probe (Biotin-Probe-m) was added to compete with labeled probe (Biotin-Probe). Biotin-probe incubated with GST protein served as the negative control

However, under Fe-deficient conditions, the leaves of the *iro2* mutants were significantly more chlorotic than the wild-type leaves (Figure 7a), which is consistent with the reported positive role of OsIRO2 in rice (Ogo et al., 2007). Next, we determined the expression levels of *OsNAS1*, *OsNAS2*, *OsYSL2*, and *OsYSL5* in the *iro2* mutants (Figure 7b). In agreement with previously reported data (Ogo et al., 2007), the *OsNAS1*, *OsNAS2*, and *OsYSL15* mRNA levels were considerably lower in the *iro2* mutants than in the wild-type control. In

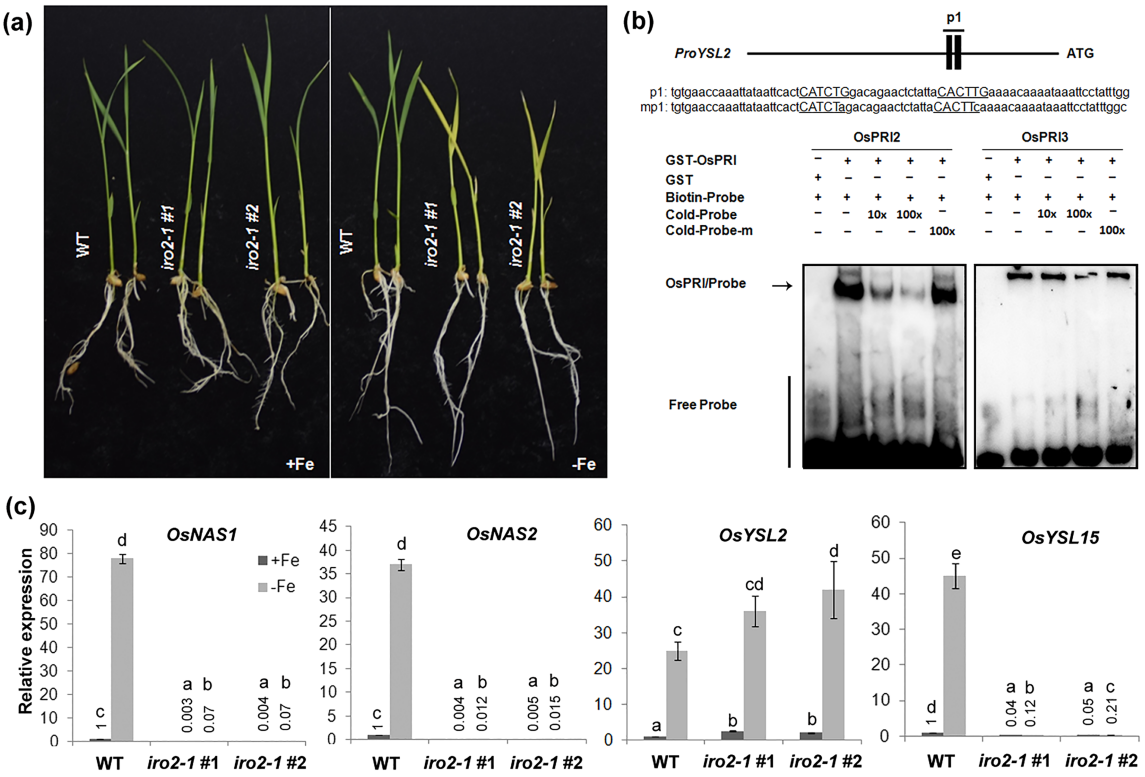

FIGURE 7 OsPRI2 and OsPRI3 bind to the promoter of *OsYSL2*. (a) Phenotypes of 10-day-old seedlings. Three-day-old seedlings germinated in wet paper were shifted to Fe-sufficient or Fe-deficient hydroponic media for 7 d. (b) Seven-day-old seedlings grown in Fe-sufficient media were transferred to Fe-sufficient or Fe-deficient media for 7 d. Roots were sampled and used for RNA extraction. The numbers above the bars indicate the corresponding mean values. Three biological replicates were performed. The different letters above each bar indicate statistically significant differences as determined by one-way ANOVA analysis followed by Tukey's multiple test ($P < 0.05$). (c) The bar indicates the position of E-boxes in the 1.5 kbp sequence from the translation start site of *OsYSL2*. The oligonucleotides (*OsYSL2-p1* and *OsYSL2-mp1*) were used as the probes. The underlined lower-case base indicates the mutated base. Each biotin-labeled DNA probe was incubated with the recombinant GST-OsPRI2/3 protein. An excess of unlabeled probe (Cold-Probe) or labeled mutated probe (Biotin-Probe-m) was added to compete with labeled probe (Biotin-Probe). Biotin-probe incubated with GST protein served as the negative control [Colour figure can be viewed at wileyonlinelibrary.com]

contrast, the *OsYSL2* mRNA level was higher in the *iro2* mutants than in the wild-type control. These data suggested that OsIRO2 is not responsible for the upregulated expression of *OsYSL2* under Fe-deficient conditions.

We also examined whether OsPRI2 and OsPRI3 directly activate the expression of *OsYSL2*. An analysis of the *OsYSL2* promoter sequence revealed two E-box motifs upstream of the transcription start site (Figure 7c). ChIP-qPCR analysis indicated that OsPRI2 and OsPRI3 were associated with the promoter of Os*YSL2* (Figure 6b). EMSA was also conducted to investigate the potential interaction of OsPRI2 and OsPRI3 with the *OsYSL2* promoter. Both OsPRI2 and OsPRI3 were able to bind to the *pYSL2-p1* fragment containing two E-boxes (Figure 7c). These data imply that OsPRI2 and OsPRI3 induce *OsYSL2* expression by directly associating with the promoter in response to Fe deficiency.

4 | DISCUSSION

The activation of Fe-deficiency responses requires a profound transcriptional reprogramming of cellular genetic programs, which involves a complex interplay between positive and negative regulators. Additionally, OsHRZ1, which is a putative Fe sensor, negatively regulates Fe homeostasis in rice (Kobayashi et al., 2013). Several transcription factors activating Fe-deficiency responses have been described, but only OsPRI1 had been identified as a direct target of OsHRZ1 (Zhang et al., 2017). However, OsPRI1 cannot be the sole target of OsHRZ1 because the *pri1 hrz1–2* double mutants are more insensitive to Fe-deficiency than the *pri1* single mutant, suggesting that there are other targets of OsHRZ1 that compensate for a loss-of-function mutation to *OsPRI1*.

The data presented herein indicate that OsPRI2 and OsPRI3 are phylogenetically closely related to OsPRI1 (Figure S1). We also confirmed that OsPRI2 and OsPRI3 physiologically interact with OsHRZ1 (Figure 1a–c). Our transient expression assays indicated that the elevated expression of OsHRZ1 promotes the degradation of OsPRI2 and OsPRI3 (Figures 1d & S2). These data suggest that OsHRZ1 promotes the degradation of OsPRI2 and OsPRI3 *in vitro*. Further investigation of their protein stability *in vivo* in response to Fe deficiency is required to explain how OsHRZ1 and OsPRI1/2/3 fine-tune Fe homeostasis in rice. To date, three proteins (OsPRI1, OsPRI2, and OsPRI3) have been identified to interact with OsHRZ1. Our unpublished work confirmed that OsPRI4 (OsbHLH57/

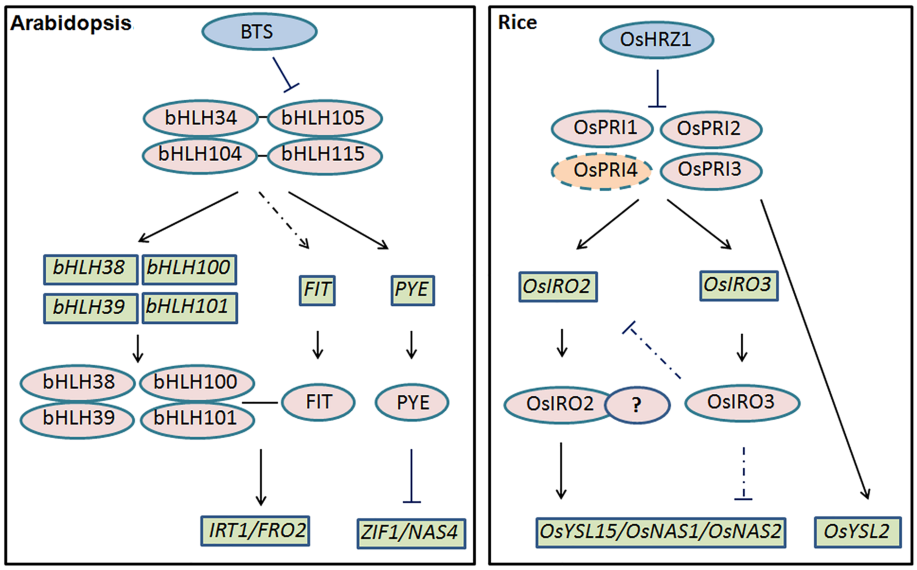

FIGURE 8 Comparison of Fe homeostasis signaling between Arabidopsis and rice. Homologue pairs, BTS=OsHRZ1, bHLH34/104/105/115 = OsPRI1/2/3/4, bHLH38/39/100/101 = OsIRO2, PYE = OsIRO3. OsPRI4 interacts with OsHRZ1 in our unpublished work. It is unclear if OsPRI4 also regulates *OsIRO2* and *OsIRO3*. The question mark indicates a potential OsIRO2 partner in rice. Arrows indicate positive regulation. Blunt arrows indicate negative regulation. Solid line, direct relationship; Dotted line, indirect relationship [Colour figure can be viewed at wileyonlinelibrary.com]

Os07g0543000), a paralog of OsPRI1 (Figure S1), interacts with OsHRZ1 in yeasts. Therefore, OsPRI4 may be the fourth target of OsHRZ1. OsHRZ2 plays a similar role to OsHRZ1 in rice (Kobayashi et al., 2013). It is possible that OsHRZ2 also interacts with and inhibits OsPRI1/2/3 to regulate Fe homeostasis in rice.

An analysis of Fe-deficiency-responsive gene expression in the *pri2* and *pri3* mutants revealed that OsPRI2 and OsPRI3 are required for the full responsiveness to Fe-deficiency. Additionally, OsPRI2 and OsPRI3 positively regulate the expression of many Fe-deficiency-responsive genes, including *OsNAS1*, *OsNAS2*, *OsYSL2*, *OsYSL15*, *OsIRO2*, and *OsIRO3* (Figures 3 & 5). Moreover, *OsIRO2* and *OsIRO3* are directly targeted by OsPRI2 and OsPRI3 (Figure 6). It is well known that OsIRO2 positively interacts with the region upstream of *OsNAS1/2* and *OsYSL15* (Ogo et al., 2007). Therefore, OsPRI2 and OsPRI3 indirectly regulate the expression of *OsNAS1*, *OsNAS2*, and *OsYSL15 via* OsIRO2. Meanwhile, OsIRO3 is a negative regulator of Fe-deficiency responses, and the overexpression of the corresponding gene inhibits the expression of *OsNAS1*, *OsNAS3*, *OsYSL15*, and *OsIRO2* (Zheng et al., 2010). The induction of *OsIRO3* expression by OsPRI2 and OsPRI3 may serve as a form of self-protection that prevents the over-accumulation of Fe. Thus, the molecular regulatory mechanism underlying Fe homeostasis is likely complex.

The *OsYSL2* gene encodes a critical Fe-nicotianamine transporter that is responsible for Fe translocation. Unlike the *OsNAS1/2* and *OsYSL15* expression levels, the expression of *OsYSL2* was not downregulated in the *iro2* mutants (Figure 7b). The direct binding of OsPRI2 and OsPRI3 to the *OsYSL2* promoter was further confirmed (Figures 6b & 7c). Therefore, OsPRI2 and OsPRI3 regulate Fe uptake by OsIRO2/3 as well as the long-distance transport of Fe by OsYSL2. *OsYSL2* is also downregulated in the *pri1* mutants, implying that it may be also a direct target of OsPRI1. We observed that both mutants and overexpression plants accumulated more Fe in the roots than the wild type plants. A previous study revealed that the downregulated expression of *OsYSL2* disrupts the Fe translocation from the roots to the shoots, resulting in increased Fe concentrations in the roots (Ishimaru et al., 2010). The expression of *OsYSL2* was considerably decreased in the *pri2* and *pri3* mutants (Figure 3), which may account for the increased root Fe accumulation. On the other hand, the Fe deficiency signal from the mutant shoots may prompt the roots to take up more Fe which was then retained in the roots of mutant plants. By contrast, the overexpression plants constitutively activated the expression of Fe uptake genes, which then caused the increased root Fe accumulation.

In this study, we generated evidence that OsPRI2 and OsPRI3 are functionally similar to OsPRI1 (Zhang et al., 2017). All three OsPRIs directly activate *OsIRO2/3* and positively regulate Fe homeostasis, indicating their similar functions. On the other hand, these proteins also appear to exhibit independent roles in responses to Fe deficiency because loss-of-function mutations to each gene impaired Fe-deficiency responses. *OsPRI2* and *OsPRI3* have different expression patterns in different organs and tissues (Figure S4), which is similar to their *A. thaliana* homologs *bHLH34/104/105/115* (Li et al., 2016; Liang et al., 2017; Zhang et al., 2015). Their different expression patterns explain why their mutants displayed different phenotypes. The expression of most of Fe-deficiency responsive genes examined was lower in the *pri3* mutants than in the *pri2* mutants (Figure 3), suggesting a greater role of OsPRI3 than OsPRI2. Given that OsPRI1/2/3 have different tissue-specific expression patterns (Figure S4), it is likely that OsPRI1/2/3 have different regulation effects on certain unknown target genes. A latest research revealed that bHLH105 negatively regulates several Fe homeostasis genes including *NAS4* which

is positively regulated by bHLH34/104/115, suggesting the divergence of their functions (Tissot et al., 2019). Further investigation is required to explore the specific functions of each OsPRI gene.

In Arabidopsis, four bHLH proteins bHLH34/104/105/115 positively regulate Fe homeostasis by regulating the expression of *bHLH38/39/100/101* (the homologues of *OsIRO2*) and PYE (the homologue of *OsIRO3*), and bHLH105/115 protein stability is negatively regulated by BTS (the homologue of OsHRZ1) (Figure 8). The expression of *OsPRI2* and *OsPRI3* is not responsive to Fe deficiency (Figure S3), suggesting that their stability may be regulated by Fe deficiency. This regulation cascade is very similar to that in rice (Figure 8). In addition, Arabidopsis bHLH34/104/105/115 can form homo- or heterodimers (Li et al., 2016; Liang et al., 2017; Zhang et al., 2015). However, we did not test if OsPRI1, OsPRI2 and OsPRI3 can form homo- or heterodimers. It is noteworthy that FIT is a key regulator of Fe homeostasis in Arabidopsis, but its rice counterpart is not found yet. In Arabidopsis, FIT regulates Fe homeostasis by direct interaction with bHLH38/39/100/101. Similarly, OsIRO2, the homolog of Arabidopsis bHLH38/39/100/101, is a key regulator of rice Fe homeostasis (Ogo et al., 2007). Therefore, it is probable that an unidentified interaction partner of OsIRO2 exists in rice (Figure 8).

OsHRZ1 is a negative regulator, and its loss-of-function causes Fe to accumulate in rice (Kobayashi et al., 2013). Consistent with the negative correlation between OsHRZ1 and OsPRI2/3, upregulated *OsPRI2* and *OsPRI3* expression levels enhance the Fe accumulation in the roots and shoots. Most Fe-biofortification strategies involve the overexpression of two or more downstream genes associated with Fe homeostasis (i.e., genes involved in chelation and transport) (Masuda, Aung, & Nishizawa, 2013). We herein reveal that the overexpression of a single gene (*OsPRI2* or *OsPRI3*) is sufficient to activate the expression of downstream genes associated with Fe uptake. Therefore, the application of OsPRI2 or OsPRI3 may be useful for developing Fe-efficient and Fe-fortified plants for improved food and biomass production.

ACKNOWLEDGEMENTS

We thank the Biogeochemical Laboratory and Central Laboratory (Xishuangbanna Tropical Botanical Garden) for assistance in the determination of metal contents. This work was supported by the Applied Basic Research Project of Yunnan Province (2017FB026), the Candidates of the Young and Middle Aged Academic Leaders of Yunnan Province (2015HB095), and the CAS 135 program (2017XTBG-T02).

CONFLICT OF INTEREST

The authors declare no conflict of interest.

ORCID

Gang Liang https://orcid.org/0000-0002-0622-4043

REFERENCES

Colangelo, E. P., & Guerinot, M. L. (2004). The essential basic helix-loop-helix protein FIT1 is required for the iron deficiency response. *The Plant Cell*, *16*, 3400–3412. https://doi.org/10.1105/tpc.104.024315

Fageria, N. K., Santos, A. B., Barbosa, F. M. P., & Guimarães, C. M. (2008). Iron toxicity in lowland rice. *Journal of Plant Nutrition*, *31*, 1676–1697.

Fisher, F., & Goding, C. R. (1992). Single amino acid substitutions alter helix-loop-helix protein specificity for bases flanking the core CANNTG motif. *EMBO Journal*, *11*, 4103–4109.

Gao, F., Robe, K., Gaymard, F., Izquierdo, E., & Dubos, C. (2019). The Transcriptional Control of Iron Homeostasis in Plants: A Tale of bHLH Transcription Factors? *Frontiers in Plant Science*, *10*, 6.

Hindt, M. N., Akmakjian, G. Z., Pivarski, K. L., Punshon, T., Baxter, I., Salt, D. E., & Guerinot, M. L. (2017). BRUTUS and its paralogs, BTS LIKE1 and BTS LIKE2, encode important negative regulators of the iron deficiency response in Arabidopsis thaliana. *Metallomics*, *9*, 876–890. https://doi.org/10.1039/c7mt00152e

Inoue, H., Higuchi, K., Takahashi, M., Nakanishi, H., Mori, S., & Nishizawa, N. K. (2003). Three rice nicotianamine synthase genes, *OsNAS1*, *OsNAS2*, and *OsNAS3* are expressed in cells involved in long-distance transport of iron and differentially regulated by iron. *Plant Journal*, *36*, 366–381. https://doi.org/10.1046/j.1365-313x.2003.01878.x

Inoue, H., Kobayashi, T., Nozoye, T., Takahashi, M., Kakei, Y., Suzuki, K., … Nishizawa, N. K. (2009). Rice OsYSL15 is an iron-regulated iron (III)-deoxymugineic acid transporter expressed in the roots and is essential for iron uptake in early growth of the seedlings. *The Journal of Biological Chemistry*, *284*, 3470–3479. https://doi.org/10.1074/jbc.M806042200

Ishimaru, Y., Masuda, H., Bashir, K., Inoue, H., Tsukamoto, T., Takahashi, M., … Nishizawa, N. K. (2010). Rice metal-nicotianamine transporter, OsYSL2, is required for the long-distance transport of iron and manganese. *Plant Journal*, *62*, 379–390. https://doi.org/10.1111/j.1365-313X.2010.04158.x

Kobayashi, T., Itai, R. N., Aung, M. S., Senoura, T., Nakanishi, H., & Nishizawa, N. K. (2012). The rice transcription factor IDEF1 directly binds to iron and other divalent metals for sensing cellular iron status. *Plant Journal*, *69*, 81–91. https://doi.org/10.1111/j.1365-313X.2011.04772.x

Kobayashi, T., Itai, R. N., Ogo, Y., Kakei, Y., Nakanishi, H., Takahashi, M., & Nishizawa, N. K. (2009). The rice transcription factor IDEF1 is essential for the early response to iron deficiency, and induces vegetative expression of late embryogenesis abundant genes. *Plant Journal*, *60*, 948–961. https://doi.org/10.1111/j.1365-313X.2009.04015.x

Kobayashi, T., Nagasaka, S., Senoura, T., Itai, R. N., Nakanishi, H., & Nishizawa, N. K. (2013). Iron-binding haemerythrin RING ubiquitin ligases regulate plant iron responses and accumulation. *Nature Communications*, *4*, 2792.

Koike, S., Inoue, H., Mizuno, D., Takahashi, M., Nakanishi, H., Mori, S., & Nishizawa, N. K. (2004). OsYSL2 is a rice metal-nicotianamine transporter that is regulated by iron and expressed in the phloem. *Plant Journal*, *39*, 415–424. https://doi.org/10.1111/j.1365-313X.2004.02146.x

Lee, S., Chiecko, J. C., Kim, S. A., Walker, E. L., Lee, Y., Guerinot, M. L., & An, G. (2009). Disruption of *OsYSL15* leads to iron inefficiency in rice plants. *Plant Physiology*, *150*, 786–800. https://doi.org/10.1104/pp.109.135418

Li, L., Gao, W., Peng, Q., Zhou, B., Kong, Q., Ying, Y., & Shou, H. (2018). Two soybean bHLH factors regulate response to iron deficiency. *Journal of Integrative Plant Biology*, *60*, 608–622. https://doi.org/10.1111/jipb.12651

Li, X., Zhang, H., Ai, Q., Liang, G., & Yu, D. (2016). Two bHLH Transcription Factors, bHLH34 and bHLH104, Regulate Iron Homeostasis in *Arabidopsis thaliana*. *Plant Physiology*, *170*, 2478–2493. https://doi.org/10.1104/pp.15.01827

Liang, G., Zhang, H. M., Li, X. L., Ai, Q., & Yu, D. (2017). bHLH transcription factor bHLH115 regulates iron homeostasis in Arabidopsis thaliana. *Journal of Experimental Botany*, *68*, 1743–1755. https://doi.org/10.1093/jxb/erx043

Liang, G., Zhang, H. M., Lou, D. J., & Yu, D. Q. (2016). Selection of highly efficient sgRNAs for CRISPR/Cas9-based plant genome editing. *Scientific Reports*, *6*, 21451.

Ling, H. Q., Bauer, P., Bereczky, Z., Keller, B., & Ganal, M. (2002). The tomato fer gene encoding a bHLH protein controls iron-uptake responses in roots. *Proceedings of the National Academy of Sciences of the United States of America*, *99*, 13938–13943.

Liu, L., Zhang, Y., Tang, S., Zhao, Q., Zhang, Z., Zhang, H., … Xie, Q. (2010). An efficient system to detect protein ubiquitination by agroinfiltration in Nicotiana benthamiana. *Plant Journal*, *61*, 893–903. https://doi.org/10.1111/j.1365-313X.2009.04109.x

Long, T. A., Tsukagoshi, H., Busch, W., Lahner, B., Salt, D. E., & Benfey, P. N. (2010). The bHLH transcription factor POPEYE regulates response to iron deficiency in Arabidopsis roots. *The Plant Cell*, *22*, 2219–2236. https://doi.org/10.1105/tpc.110.074096

Masuda, H., Aung, M. S., & Nishizawa, N. K. (2013). Iron biofortification of rice using different transgenic approaches. *Rice (N Y)*, *6*, 40.

Muckenthaler, M. U., Galy, B., & Hentze, M. W. (2008). Systemic iron homeostasis and the iron-responsive element/iron-regulatory protein (IRE/IRP) regulatory network. *Annual Review of Nutrition*, *28*, 197–213. https://doi.org/10.1146/annurev.nutr.28.061807.155521

Neue, H. U., Quijano, C., Senadhira, D., & Setter, T. (1998). Strategies for dealing with micronutrient disorders and salinity in lowland rice systems. *Field Crops Research*, *56*, 139–155.

Ogo, Y., Itai, R. N., Kobayashi, T., Aung, M. S., Nakanishi, H., & Nishizawa, N. K. (2011). OsIRO2 is responsible for iron utilization in rice and improves growth and yield in calcareous soil. *Plant Molecular Biology*, *75*, 593–605. https://doi.org/10.1007/s11103-011-9752-6

Ogo, Y., Itai, R. N., Nakanishi, H., Kobayashi, T., Takahashi, M., Mori, S., & Nishizawa, N. K. (2007). The rice bHLH protein OsIRO2 is an essential regulator of the genes involved in Fe uptake under Fe-deficient conditions. *Plant Journal*, *51*, 366–377. https://doi.org/10.1111/j.1365-313X.2007.03149.x

Quinet, M., Vromman, D., Clippe, A., Bertin, P., Lequeux, H., Dufey, I., … LefèVre, I. (2012). Combined transcriptomic and physiological approaches reveal strong differences between short- and long-term response of rice (Oryza sativa) to iron toxicity. *Plant, Cell and Environment*, *35*, 1837–1859.

Römheld, V., & Marschner, H. (1986). Evidence for a specific uptake system for iron phytosiderophores in roots of grasses. *Plant Physiology*, *80*, 175–180.

Salahudeen, A. A., Thompson, J. W., Ruiz, J. C., Ma, H. W., Kinch, L. N., Li, Q., … Bruick, R. K. (2009). An E3 ligase possessing an iron-responsive hemerythrin domain is a regulator of iron homeostasis. *Science*, *326*, 722–726. https://doi.org/10.1126/science.1176326

Saleh, A., Alvarez-Venegas, R., & Avramova, Z. (2008). An efficient chromatin immunoprecipitation (ChIP) protocol for studying histone modifications in Arabidopsis plants. *Nature Protocols*, *3*, 1018–1025. https://doi.org/10.1038/nprot.2008.66

Selote, D., Samira, R., Matthiadis, A., Gillikin, J. W., & Long, T. A. (2015). Iron-binding E3 ligase mediates iron response in plants by targeting basic helix-loop-helix transcription factors. *Plant Physiology*, *167*, 273–286. https://doi.org/10.1104/pp.114.250837

Takagi, S. (1976). Naturally occurring iron-chelating compounds in oat- and rice-root washing. I. Activity measurement and preliminary characterization. *Soil Science and Plant Nutrition*, *22*, 423–433.

Tissot, N., Robe, K., Gao, F., Grant-Grant, S., Boucherez, J., Bellegarde, F., … Dubos, C. (2019). Transcriptional integration of the responses to iron availability in Arabidopsis by the bHLH factor ILR3. *New Phytologist*, *223*, 1433–1446. https://doi.org/10.1111/nph.15753

Vashisht, A. A., Zumbrennen, K. B., Huang, X., Powers, D. N., Durazo, A., Sun, D., … Wohlschlegel, J. A. (2009). Control of iron homeostasis by an iron-regulated ubiquitin ligase. *Science*, *326*, 718–721. https://doi.org/10.1126/science.1176333

Wang, F., Zhu, D., Huang, X., Li, S., Gong, Y., Yao, Q., … Deng, X. W. (2009). Biochemical insights on degradation of Arabidopsis DELLA proteins gained from a cell-free assay system. *The Plant Cell*, *21*, 2378–2390. https://doi.org/10.1105/tpc.108.065433

Wang, H. Y., Klatte, M., Jakoby, M., Bäumlein, H., Weisshaar, B., & Bauer, P. (2007). Irondeficiency-mediated stress regulation of four subgroup Ib BHLH genes inArabidopsis thaliana. *Planta*, *226*, 897–908.

Wang, N., Cui, Y., Liu, Y., Fan, H., Du, J., Huang, Z., … Ling, H. Q. (2013). Requirement and functional redundancy of Ib subgroup bHLH proteins for iron deficiencyresponses and uptake in Arabidopsis thaliana. *Molecular Plant*, *6*, 503–513.

Xie, X., Ma, X., Zhu, Q., Zeng, D., Li, G., & Liu, Y. G. (2017). CRISPR-GE: A Convenient Software Toolkit for CRISPR-Based Genome Editing. *Molecular Plant*, *10*, 1246–1249. https://doi.org/10.1016/j.molp.2017.06.004

Yuan, Y., Wu, H., Wang, N., Li, J., Zhao, W., Du, J., … Ling, H. Q. (2008). FIT interacts with AtbHLH38 and AtbHLH39 in regulating iron uptake gene expression for iron homeostasis in Arabidopsis. *Cell Research*, *18*, 385–397. https://doi.org/10.1038/cr.2008.26

Yuan, Y., Zhang, J., Wang, D. W., & Ling, H. Q. (2005). AtbHLH29 of Arabidopsis thaliana is a functional ortholog of tomato FER involved in controlling iron acquisition in strategy I plants. *Cell Research*, *15*, 613–621. https://doi.org/10.1038/sj.cr.7290331

Zhang, H., Li, Y., Yao, X., Liang, G., & Yu, D. (2017). POSITIVE REGULATOR OF IRON HOMEOSTASIS1, OsPRI1, Facilitates Iron Homeostasis. *Plant Physiology*, *175*, 543–554.

Zhang, J., Liu, B., Li, M., Feng, D., Jin, H., Wang, P., … Wang, H. B. (2015). The bHLH Transcription Factor bHLH104 Interacts with IAA-LEUCINE RESISTANT3 and Modulates Iron Homeostasis in Arabidopsis. *The Plant Cell*, *27*, 787–805. https://doi.org/10.1105/tpc.114.132704

Zhao, Q., Ren, Y. R., Wang, Q. J., Wang, X. F., You, C. X., & Hao, Y. J. (2016). Ubiquitination-Related MdBT Scaffold Proteins Target a bHLH Transcription Factor for Iron Homeostasis. *Plant Physiology*, *172*, 1973–1988. https://doi.org/10.1104/pp.16.01323

Zhao, Q., Ren, Y. R., Wang, Q. J., Yao, Y. X., You, C. X., & Hao, Y. J. (2016). Overexpression of MdbHLH104 gene enhances the tolerance to iron deficiency in apple. *Plant Biotechnology Journal*, *14*, 1633–1645.

Zheng, L., Ying, Y., Wang, L., Wang, F., Whelan, J., & Shou, H. (2010). Identification of a novel iron regulated basic helix-loop-helix protein involved in Fe homeostasis in Oryza sativa. *BMC Plant Biology*, *10*, 166.

SUPPORTING INFORMATION

Additional supporting information may be found online in the Supporting Information section at the end of the article.

Figure S1. Alignment of protein sequences.

Figure S2. Degradation of OsPRI2/3 promoted by OsHRZ1

Figure S3. Expression of *OsPRI2* and *OsPRI3* in response to Fe deficiency.

Figure S4. Tissue-specific expression pattern of OsPRI2/3.

Figure S5. Root and shoot length and seed Fe concentration of *pri2* and *pri3* mutants.

Figure S6. Identification of overexpression plants.

Figure S7. Root and shoot length and seed Fe concentration of overexpression plants.

Figure S8. Mutation in the *iro2* mutants.

Table S1. Primers used in this paper.

How to cite this article: Zhang H, Li Y, Pu M, Xu P, Liang G, Yu D. *Oryza sativa* POSITIVE REGULATOR OF IRON DEFICIENCY RESPONSE 2 (OsPRI2) and OsPRI3 are involved in the maintenance of Fe homeostasis. *Plant Cell Environ*. 2019;1–14. https://doi.org/10.1111/pce.13655